



Ultra-widefield Imaging of the Peripheral Retinal Vasculature in Normal Subjects

Michael Singer, MD, PhD,^{1,*} Min Sagong, MD, PhD,^{2,3,*} Jano van Hemert, PhD,⁴ Laura Kuehlewein, MD,^{2,5} Darren Bell, MD,¹ Srinivas R. Sadda, MD²

Purpose: To establish the extent of the peripheral retinal vasculature in normal eyes using ultra-widefield (UWF) fluorescein angiography.

Design: Prospective, observational study.

Participants: Fifty-nine eyes of 31 normal subjects, stratified by age, with no evidence of ocular disease in either eye by history and ophthalmoscopic examination.

Methods: Ultra-widefield fluorescein angiographic images were captured centrally and with peripheral steering using the Optos 200Tx (Optos, Dunfermline, United Kingdom). Images obtained at different gaze angles were montaged and corrected for peripheral distortion using a stereographic projection method to provide a single image for grading of the peripheral edge of the visible vasculature. The border of the vascularized retina was expressed as a radial surface distance from the center of the optic disc. The vascularized area was calculated based on this mean peripheral border position for each quadrant.

Main Outcome Measures: Mean distance (mm) from the center of optic disc to the peripheral vascular border.

Results: In normal eyes, the mean radial surface distance from the center of the optic disc to the peripheral edge of the visible vasculature was 20.3 ± 1.4 mm and the mean area of normal perfused retina was 977.0 mm^2 . There was no significant difference between right and left eyes or between male and female participants. However, the distance to the periphery differed depending on the quadrant, with temporal (22.5 ± 0.9 mm) being larger than inferior (20.4 ± 1.7 mm) being larger than superior (19.2 ± 1.5 mm) being larger than nasal (17.4 ± 0.9 mm; $P < 0.001$) for all interquadrant comparisons. Interestingly, the distances to the perfused vascular border were significantly shorter in older individuals (≥ 60 years) than in younger subjects.

Conclusions: Ultra-widefield fluorescein angiography is an important tool for studying the extent of peripheral retinal vasculature. With the increasing use of UWF imaging to evaluate and manage patients with retinal vascular disease, the normative data from this study may provide a useful reference when assessing the pathologic significance of findings in the setting of disease. *Ophthalmology* 2016;■:1–7 © 2016 by the American Academy of Ophthalmology.

The introduction of ultra-widefield (UWF) imaging systems has had a significant impact on the diagnosis and management of various retinal disorders. The UWF imaging provides up to a 200° view of the retina in a single capture and allows detection of peripheral pathologic features that can be missed on the 7 standard fields of the Early Treatment Diabetic Retinopathy Study.^{1–6} Identification of peripheral retinal nonperfusion is thought to be of importance for the management of eyes with retinal vascular diseases such as retinal vein occlusion and diabetic retinopathy.^{6–11} Several studies have demonstrated that the extent of retinal nonperfusion was associated with the severity of macular edema and with its resolution after treatment.^{7–9} These studies also suggest that retinal nonperfusion is related to the upregulation of vascular endothelial growth factor caused by hypoxia.^{8,9}

The single, centered image used by previous investigators captures a maximum of 80% of the fundus, but includes an inevitable nonlinear distortion caused by the

elliptical mirror used in the Optos UWF system (Optos, Dunfermline, United Kingdom).^{1–11} In addition, these previous studies were unable to determine the precise size of the nonperfused area, because there was no solution at that time to resolve the inherent peripheral distortion present in large-field fundus images. They quantified the severity or extent of nonperfusion by expressing the number of pixels within an area of nonperfusion as a percentage of the number of pixels seen within the total visible retina (ischemic index).^{7–11} However, the total visible retina also can include the physiologic peripheral nonperfused area near the ora serrata just beyond the normal vascular terminus. Ideally, to depict the extent of pathologic nonperfusion most accurately, this physiologic nonperfusion area should be excluded from the total visible retina when computing the ischemic index. This is particularly important because the total visible retina may vary from case to case depending on limitations of image acquisition.

An understanding of the normal peripheral vasculature is particularly important, given the recent increase in multicenter, randomized clinical trials such as Diabetic Retinopathy Clinical Research Network protocol AA (designed to assess the impact of peripheral lesions on diabetic retinopathy severity and progression) and the Study of Comparative Treatments for Retinal Vein Occlusion 2, which aims to evaluate the impact of treatment on peripheral nonperfusion.

Recent advances in UWF imaging hardware and software have made accurate quantification of the normal perfused retina now possible. Stereographic projection software, now available in commercial UWF devices, allows images obtained at different gaze angles to be montaged and corrected for peripheral distortion. Using this software, researchers can calculate the anatomically correct areas of nonperfusion in metric units using spherical trigonometry, rather than expressing the area as a percentage.¹² Our previous study showed that this quantification methodology can generate accurate retinal measurements in a human eye using a retinal prosthesis as an *in vivo* reference standard.¹³

We sought to develop a database of the extent of the peripheral retinal vasculature in actual anatomic units (millimeters) in normal eyes using UWF fluorescein angiography (FA). We also evaluated the change of the extent of perfused retina, with stratification controlled for age.

Methods

Study Population

This prospective observational study was conducted at Medical Center Ophthalmology Associates, San Antonio, Texas, and was approved by its institutional review board. This study adhered to the tenets of the Declaration of Helsinki. Written informed consent was obtained from all subjects before imaging.

The normal subjects were recruited for standardized UWF FA using an Optos 200Tx device with age stratification by decade. All subjects underwent detailed clinical examinations including autorefractometry, visual acuity, intraocular pressure measurement, slit-lamp examination, ophthalmoscopy, and optical coherence tomography. Subjects were eligible for inclusion if they were older than 20 years with no known retinal or systemic diseases. The main exclusion criteria included the following: age younger than 20 or older than 80 years; contraindication to dilation; presence of retinal or optic nerve disease, including glaucoma; past history of vitreoretinal surgery; any ocular condition that would interfere with good-quality image acquisition, such as corneal opacities, cataract, or dense vitreous hemorrhage; any medical condition that might interfere with the subject's compliance with study procedures, such as ataxia or nystagmus, that could affect the subject's ability to maintain steady head or eye positioning; a history of diabetes, high blood pressure, or vascular diseases (cardiovascular, peripheral vascular, or cerebrovascular); or the use of vasodilators. Pregnant women or those who might be pregnant also were excluded from participation.

Widefield Image Acquisition and Quantification

Subject eyes were dilated with tropicamide 1% and phenylephrine 2.5%, and UWF pseudocolor images were captured, centered on the fovea, and steered peripherally (nasally, temporally, superiorly, inferiorly). After intravenous administration of fluorescein dye, UWF FA images were obtained during the early (45 seconds), middle (2 minutes and 30 seconds), and late (5 minutes) phases of

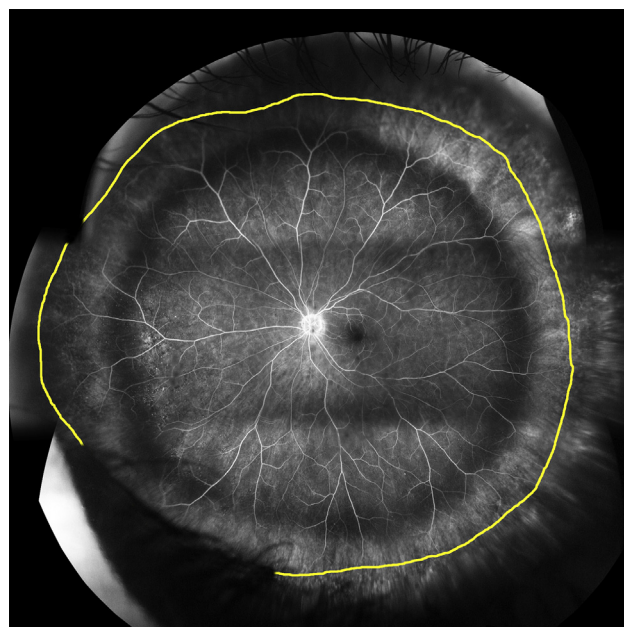


Figure 1. Ultra-widefield fluorescein angiogram image after stereographic projection and montage of central, superior-steered, and inferior-steered images. The extent of peripheral retinal vasculature has been defined by the grader by demarcating (yellow line) the peripheral extent of the blood vessel arborization (the junction between the vascularized and non-vascularized retina).

the angiography. At the 3 time points, in addition to a central image centered on the macula, the FA images were steered superiorly, inferiorly, temporally, and nasally to allow clear visualization of the peripheral edge of the visible vasculature.

Uncorrected raw images were exported from the device and sent to the Doheny Image Reading Center, Doheny Eye Institute, Los Angeles, California. All images for each subject were transformed to stereographic projection images using proprietary prototype software available from the manufacturer. This software is now available in the commercial device or product. This projection technique was accomplished by ray tracing every pixel through a combined optical model of the Optos 200Tx and a Navarro UWF model eye with an axial length of 24 mm.¹⁴ This optical model represented the projection used by the Optos 200Tx scanning laser ophthalmoscopy platform to create the 2-dimensional optomap. The software also allowed the grader to register the 4 steered images to the on-axis image automatically to create a montage of all images (by adding each image one by one). Image registration between a pair of images first extracted their vasculature and subsequently applied rotational affine translation with cross-correlation (i.e., an algorithm slightly rotated the peripheral images to align vasculature). Finally, segments were blended together to create a contiguous montage. Because angiographic images were obtained at 3 time points (early, middle, and late), a separate montage was created for each time point. All montage images then were graded independently by a trained reading center—certified ophthalmologist (M.S.) who was masked to the patient's clinical data, including age and gender. Using ImageJ version 1.49b (ImageJ version 1.49b; US National Institutes of Health, Bethesda, MD) the graders manually outlined the peripheral extent of the blood vessel arborization (the junction between the vascularized and nonvascularized retina; Fig 1). Because the small-vessel detail is expected to be best at the early time point, the graders generally chose the early montage for assessments, zoomed in to the peripheral retina, and panned for 360°

while adjusting brightness and contrast. If the border was unclear at any sector location, the graders used the montage images from other time points to refine the assessment. Sectors in which the border could not be seen clearly even at the other time points were left unsegmented. Grading was repeated by a second independent masked certified Doheny Image Reading Center grader (L.K.). Each pixel annotated as the border of the vascularized retina in the montage images was bordered individually to its anatomically correct location on the 3-dimensional model eye, and spherical trigonometry was applied (using the Optos software) to calculate its respective radial distance and surface area at each quadrant (superior, nasal, inferior, temporal) from the center of the optic disc in metric units. The disc center was defined as the anatomic center of the optic nerve head. The difference in the vascular border by the same grader and between graders at each meridian was evaluated (see below) to assess grading reproducibility. However, to generate a single result for each case for quantitative comparisons between subjects and to compute a mean for all subjects, the graders met in open adjudication to arrive at a single consensus position for this border at every location for each subject.

Data Analysis

As noted in “Methods,” graders left unsegmented any regions or segments in which the border could not be defined for individual cases. This would be expected to leave the map of the normal perfused retina discontinuous or incomplete. However, within particular subgroups (e.g., men or subjects within certain age ranges), the results for subjects could be combined to result in a complete map, with a mean result and a 95% confidence interval around the border position at each meridian or clock hour.

Intereye differences (right and left eyes) and differences in mean distances from fovea to peripheral vascular border between female and male individuals were examined with the independent *t* test and paired *t* test. A 1-way analysis of variance test was used to compare mean distances among the 4 quadrants with post hoc analysis using Dunnett’s test. Kruskal-Wallis tests were used to compare the 6 different age groups (20–29 years, 11 eyes; 30–39 years, 10 eyes; 40–49 years, 9 eyes; 50–59 years, 10 eyes; 60–64 years, 8 eyes; ≥65 years, 11 eyes) on mean distance in each meridian. The Mann–Whitney *U* test was used in pairwise comparisons between the age groups. Interclass correlation coefficients (ICCs) and similarity indices were calculated to evaluate intra-grader and intergrader reproducibility. The Jaccard and Dice similarity indices used in this study are direct measurements of the pixel overlap of the areas annotated by each grader. With the ICC alone, 2 graders could have annotated completely differently shaped regions, but still have produced a small mean difference with a high correlation, whereas the Jaccard and Dice similarity indices would cause poor agreement in such a scenario. Statistical analyses were performed using SPSS software version 16.0 (SPSS, Inc, Chicago, IL).

Results

Fifty-nine eyes of 31 subjects were included in the quantitative analysis. Two eyes were excluded because the most peripheral end of the vasculature was not observed in any sector. One eye was excluded because a pigmented lesion obscured the demarcation of the peripheral vascular border. Thirteen subjects (41.9%) were men and 18 (58.1%) were women, with a mean age of 47.1 years (range, 20–77 years; standard deviation, ±16.8 years). Most subjects were white (27 subjects; 87.1%); 1 subject was Latino, 1 subject was Asian, and 2 subjects were black. Of 59 eyes, 56 eyes (94.9%) were phakic and 3 eyes (5.1%) were pseudophakic. The mean

Table 1. Mean Radial Surface Distance from the Center of Optic Disc to the Peripheral Vascular Border in Normal Subjects

	Mean Distance (mm)	P Value
Laterality		
Right eye	20.2±1.4	0.269
Left eye	20.4±1.3	
Gender		
Male	20.5±1.3	0.355
Female	20.2±1.4	
Quadrant		
Superior	19.2±1.5	<0.001 (for all interquadrant comparisons*)
Inferior	20.4±1.7	
Nasal	17.4±0.9	
Temporal	22.5±0.9	

Data are mean ± standard deviation unless otherwise indicated.

*One-way analysis of variance with post hoc analysis using Dunnett’s *t* test.

spherical equivalent was -1.01 diopters (D; median, -0.50 D; standard deviation, ± 2.09 D), whereas the range varied from -9.75 D to $+2.00$ D.

Extent of Normal Perfused Retina

The mean area of total perfused retina was 977.0 mm². With the center of the optic disc used as the reference point, there was no significant difference in the mean distances to the peripheral border of the retinal vasculature between the right eye (20.2 ± 1.4 mm) and the left eye (20.4 ± 1.3 mm) or between the men (20.5 ± 1.3 mm) and women (20.2 ± 1.4 mm; $P = 0.269$ and $P = 0.355$, respectively). Mean distance from the disc center to the peripheral vascular border was significantly different depending on the quadrant, with temporal distances (22.5 ± 0.9 mm) being greater than inferior distances (20.4 ± 1.7 mm) being greater than superior distances (19.2 ± 1.5 mm) being greater than nasal distances (17.4 ± 0.9 mm; $P < 0.001$ for all interquadrant comparisons; Table 1). A complete map of the normal border (mean distance and 95% confidence interval) was constructed by overlapping defined borders across the cohort. Left eyes were transposed or flipped to match right eyes (Fig 2A). After the normal perfused retina was defined based on this normal border, the level of ischemia in retinal vascular diseases could be defined based on the amount of perfused retina present in an eye compared with the total visible retina. Figure 3 shows a significant difference between ischemic index based on total visible retina and that based on normal perfused retina in a patient with central retinal vein occlusion. Despite the use of montages, in 24 of 59 eyes (40.7%), graders could not mark the border of the peripheral retinal vasculature because of lash artifact or because the most peripheral end of the vasculature extended beyond the range of montage in at least 1 quadrant (1 quadrant, 17 eyes; 2 quadrants, 5 eyes; 3 or more quadrants, 2 eyes). Interestingly, in younger subjects (<60 years), there was a higher frequency of unsegmented border of the peripheral vasculature in at least 1 quadrant than there was in older subjects (19 of 40 eyes [47.5%] vs. 5 of 19 eyes [26.3%]; $P = 0.122$).

Variations in Normal Perfused Retina According to Age

Pairwise comparisons between different age groups showed that the mean distance from the disc center to peripheral vascular border of 2 older groups (60–64 years and 65 years and older) was

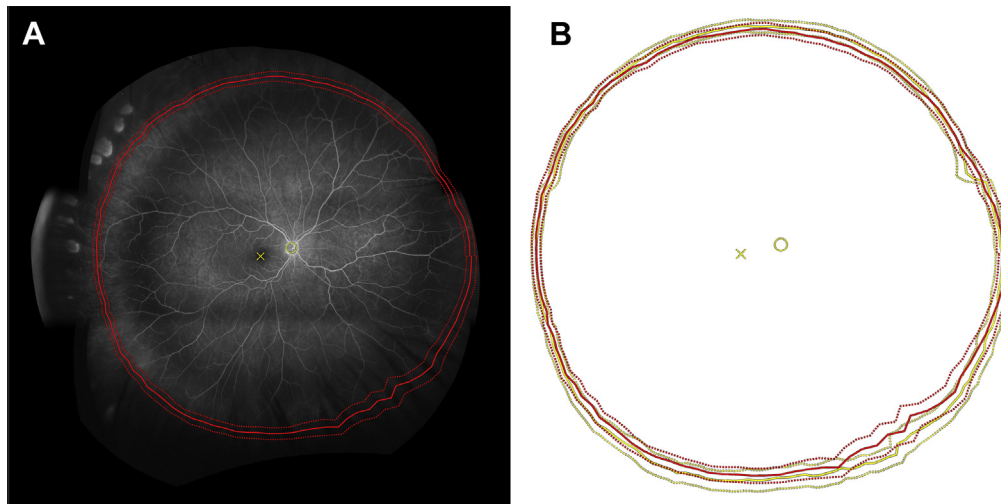


Figure 2. **A**, Virtual map of the border of the normal perfused retina (solid red line, mean position; dotted red lines, 95% confidence intervals) constructed by overlapping defined borders across the cohort, after transposing the left eyes to the right eyes to allow superimposition. The center of the optic nerve head was used to center images, and the center of the fovea was used to ensure consistent rotation. **B**, Superimposed virtual maps of the normal perfused border of the cohort as determined by 2 independent masked graders (grader 1 in red, grader 2 in yellow). Note the extensive overlap highlighting the high level of intergrader agreement.

significantly shorter than those of the other age groups (20–29 years, 30–39 years, 40–49 years, and 50–59 years). Overall, the older subjects (≥ 60 years) demonstrated a significantly shorter mean distance to the vascular border compared with those younger than 60 years ($P < 0.001$). Meanwhile, in normal subjects 20 to 60 years of age, the mean distance from the disc center to peripheral vascular border showed no significant difference with age (20–29 years, 21.3 ± 1.1 mm; 30–39 years, 21.0 ± 0.9 mm; 40–49 years, 20.8 ± 1.2 mm; and 50–59 years, 20.9 ± 0.9 mm). There was no significant difference in mean distance to the border between subjects 60 to 64 years of age and those who were 65 years of age or older. However, the study was not powered to detect small differences. This tendency toward a shorter distance between the

disc center and the vascular border in subjects 60 years of age or older was observed in all quadrants (Table 2).

Intraobserver and Interobserver Agreement

Intragrader agreement (M.S.) for the mean radial distance from the disc center to the peripheral vascular border was excellent, with an ICC of 0.968 (superior, 0.959; inferior, 0.967; temporal, 0.972; and nasal, 0.971). Intergrader agreement for the mean distance was also excellent, with an ICC of 0.954 (superior, 0.948; inferior, 0.966; temporal, 0.955; and nasal, 0.953). The Jaccard and Dice similarity indices, which evaluate the degree of pixel overlap, were 0.87 and 0.81, suggesting a high intergrader agreement (Fig 2B).

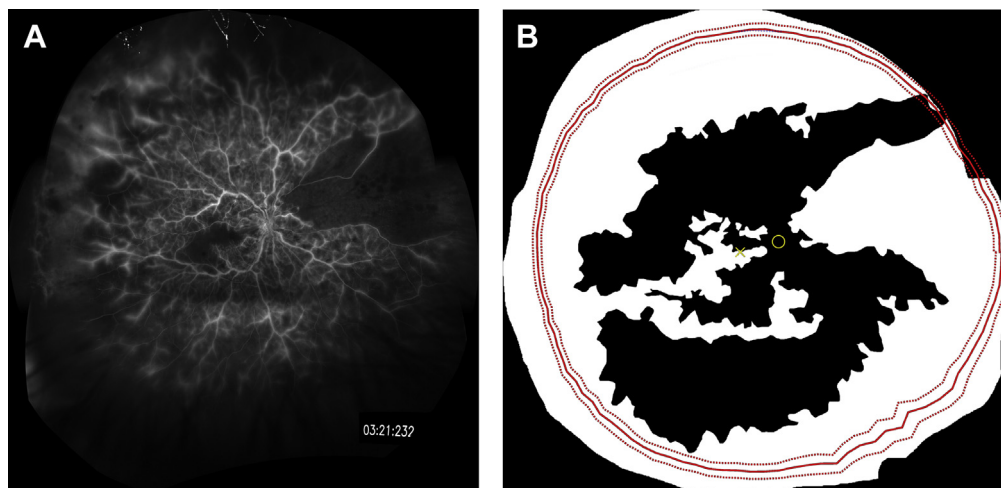


Figure 3. **A**, Montaged wide-field fluorescein angiographic image from a patient with central retinal vein occlusion. **B**, Grading diagram illustrating the areas of perfused retina (shaded black) and nonperfused retina (shaded white) based on the total visible retina. The superimposed red lines reflect the mean border (solid red line; 95% confidence intervals shown as dotted lines) of perfused retina based on the normal cohort. Only the areas of nonperfusion within the red circle are considered pathologic. Calculating the ischemic index based on the normal perfused retina as opposed to total visible retina reduces the value from 51.1% to 46.8%.

Table 2. Changes in Mean Distance from the Center of Optic Disc to the Border of the Peripheral Vasculature According to Age in Normal Subjects

Sector	Mean Distance (mm) by Age Range (yrs)						P Value*
	20–29	30–39	40–49	50–59	60–64	65+	
Superior	20.3±1.1 (n = 11 eyes)	19.6±1.4 (n = 9 eyes)	19.8±1.3 (n = 8 eyes)	19.9±0.9 (n = 10 eyes)	17.8±1.0 (n = 8 eyes)	17.9±0.9 (n = 11 eyes)	<0.001
Inferior	20.9±1.1 (n = 10 eyes)	20.7±1.4 (n = 10 eyes)	21.1±0.9 (n = 7 eyes)	21.7±1.0 (n = 6 eyes)	19.1±1.3 (n = 8 eyes)	18.9±2.5 (n = 6 eyes)	0.007
Nasal	17.8±0.8 (n = 5 eyes)	17.8±0.7 (n = 9 eyes)	17.3±0.9 (n = 5 eyes)	17.9±0.8 (n = 8 eyes)	17.0±0.9 (n = 8 eyes)	16.7±0.6 (n = 11 eyes)	0.010
Temporal	22.9±0.6 (n = 11 eyes)	23.1±0.7 (n = 10 eyes)	22.5±0.7 (n = 9 eyes)	23.0±0.4 (n = 10 eyes)	21.3±1.0 (n = 8 eyes)	21.8±0.7 (n = 11 eyes)	<0.001
Mean	21.3±1.1 (n = 11 eyes)	21.0±0.9 (n = 10 eyes)	20.8±1.2 (n = 9 eyes)	20.9±0.9 (n = 10 eyes)	18.8±0.9 (n = 8 eyes)	19.0±0.7 (n = 11 eyes)	<0.001

Data are mean ± standard deviation unless otherwise noted. Post hoc analysis (pairwise comparison using Mann–Whitney *U* test) revealed that mean distance was significantly shorter in older patients (20–29 yrs, 30–39 yrs, 40–49 yrs, 50–59 yrs vs. 60–64 yrs, ≥65 yrs; all *P* < 0.05).

*Statistical significance was calculated by the Kruskal-Wallis test.

Discussion

In the present study, we evaluated the extent of normal perfused retina with new software (now available on the commercial device) using stereographic projection, which allows correction of inherent peripheral distortion and permits montaging of the central and steered UWF images as well as accurate measurement of structures. With the center of the optic disc as the reference point, mean area and distance to the peripheral vascular border were 977.0 mm² and 20.3±1.4 mm. There was no difference in the extent of normal perfused retina between both eyes in men and women. However, there were significant differences in the different quadrants with the order of temporal, inferior, superior, and nasal, with the distance being greatest in the temporal quadrant. Interestingly, the distances to the perfused vascular border were significantly shorter in individuals 60 years of age or older compared with younger subjects. This tendency was observed in all quadrants.

Thus far, UWF images have presented a significant challenge for obtaining quantitative measurements because they inherently include significant nonlinear distortion when projected onto a 2-dimensional surface for viewing.^{12,15,16} Two lesions with similar size on an uncorrected image may differ significantly in actual area, depending on whether they are located more centrally or more peripherally.^{12,16} This distortion could result in overestimation of the size of a peripheral lesion. Ophthalmologists have used reference structures in the posterior pole to estimate the size of other objects in the fundus. For instance, previous studies have converted areas measured in pixels into square millimeters by assessing the number of pixels in central landmarks such as the optic disc¹⁰ or the retinal vein diameter at the margin of the disc¹⁵ for the purpose of clinical interpretation. However, these methods do not account for peripheral distortion of the UWF images. In addition, the sizes of the landmarks vary from one person to another; thus, such conversion strategies are not accurate.¹⁷ The stereographic projection used in this study provides a conformal 2-dimensional image-preserving shape mapped

by ray tracing all relevant pixels from a 3-dimensional model.¹² This technique produces a montage by registering the 4 eye-steered stereographic projected images on the on-axis image and allows anatomically correct measurements of the perfused retina on the montage image.¹² Using montaged images is crucial for the assessments described in this study, because it can help mitigate lash artifact, particularly in the inferior quadrant. The latest generation of UWF imaging devices (Optos California, Daytona, and 200Tx) include automated software tools for stereographic projection and registration that facilitate interdevice measurement comparisons.

In the normal eye, the retinal capillaries that do not reach the far peripheral area (ora serrata) of the fundus often are observed by ophthalmoscopy. Rutnin and Schepens¹⁸ reported the presence of an area of 0.5 disc diameter (DD) of peripheral nonperfusion in normal adults on ophthalmoscopic examination. Asdourian and Goldberg¹⁹ used astigmatic FA to show the presence of approximately 1 mm (0.67 DD) of peripheral nonperfusion in 12 healthy young adults with no ocular pathologic features. In full-term neonates, the extent of the retinal vasculature is variable, especially temporally and superiorly, where the peripheral avascular zone may be up to 1.5 mm in width.²⁰ Blair et al²¹ investigated the peripheral nonperfused retinal area in 23 children, ranging in age from 2 months to 13 years, using the RetCam system (Clarity Medical Systems, Pleasanton, CA). They reported that no ocular pathologic features were found, but the overall mean width of retinal nonperfusion in these eyes was 1.50 DD or less, with a mean of 0.6 DD nasally and 0.9 DD temporally. This region of normal peripheral nonperfusion is not surprising because the far peripheral retina is very thin and likely can be oxygenated adequately by the underlying choroid. This is thought to be the mechanism of partial vision preservation or recovery in patients with severe central retinal artery occlusion.²² Spitznas and Bornfeld²³ investigated the architecture of the most peripheral retinal vessels histologically in enucleated eyes or in those obtained at autopsy, and they reported that the number of

small vessels in the periphery was fewer and that the distribution of vessels was reduced to a single retinal layer, that is, the retinal ganglion cell layer or the nerve fiber layer. They suggested that the peripheral vasculature was confined to a single layer because of the thinness of the peripheral sensory retina.²³ In addition to the thin peripheral retina, the more superficial location of vessels allowed the boundary between nonperfused and perfused retina to be observed more clearly in the far periphery by UWF FA. These points can facilitate actual measurement of normal perfused retina using the stereographic projection and montaging method.

The mean area of perfused retina in the present study was 977.0 mm². When considering that this result contains only perfused retina, it is compatible with total retinal area of 1133.8 mm² calculated by Taylor and Jennings.²⁴ In addition, we constructed a complete map of the normal perfused retinal border (mean distance from the disc center) by overlapping defined borders across the cohort (Fig 2A). This map of the normal perfused retina may have potential applications in quantitative studies of retinal vascular diseases, which have been reporting results as ischemic or leaking indices.^{7–11,25} These indices currently are calculated by expressing the areas of retinal nonperfusion or leakage as a percentage of the total area. The total area has been defined variably as a total visible retinal area^{7–9} or an area where retinal vasculature is in sharp focus,^{10,25} thereby allowing accurate visualization of smaller retinal capillaries. However, the area of visible retina has demonstrated a large range of variability, including a range of 559.4 to 797.7 mm² in one study (without using steering).¹⁶ This variability calls into question the validity of using this method to assess areas of nonperfusion or leakage. A major issue in assessment of UWF is that the images may vary across subjects and even in the same subject during follow-up examinations. In a study evaluating the association of UWF FA retinal nonperfusion with diabetic retinopathy severity and the presence of peripheral lesions, Silva et al²⁶ reported that nonperfusion was located predominantly in the far periphery with a low ischemic index of approximately 15%. This underlines the necessity of the exclusion of normal peripheral nonperfused retina, which can be considered as physiologic nonperfusion, when assessing the total area. Interestingly, our study showed that normal perfused retina is smaller in the subjects 60 years of age and older than in younger subjects, in all quadrants. This suggests that there may be a need to adjust the reference for normal perfused retinal area depending on the age, although this observation clearly requires confirmation in a larger study with more subjects in the various age groups.

When assessing the results of our study, it is important also to consider its limitations. First, the sample size is still relatively small, particularly when considering specific age groups. As a result, our study was underpowered to detect small differences between groups. Second, because we excluded patients with hypertension (or any systemic disease), our findings may not be applicable to older patients who are otherwise healthy except for hypertension, which is of course very common in elderly patients. Third, we were not able to obtain axial lengths in all subjects, and thus we

were not able to correct measurements for axial length in this analysis.^{13,16} Fourth, eyes with an unsegmented border of the peripheral vasculature in at least 1 quadrant were more frequent in the subjects 60 years of age or younger than in the older subjects, presumably because these younger subjects had a greater distance to the vascularized border. However, this means that the area of the normal perfused retina of younger subjects reported in our study may actually still be an underestimate.

Despite the above limitations, our study still has several strengths, including its prospective design; the use of experienced, independent reading center graders; and a demonstrated high level of grading reproducibility. In addition, unlike previous FA studies that have used the normal eyes of patients with unilateral retinal diseases as a control,²⁷ we included only subjects in whom both eyes were normal.

In summary, the stereographic projection algorithm used in this study enabled standardized montages with correction of peripheral distortion and accurate quantification of the vascularized retina from UWF images. Using this approach, we were able to define the extent of normal peripheral retinal vasculature and the area of normal perfused retina. The findings from this normative study may provide a useful reference when assessing the pathologic significance of nonperfusion in the setting of retinal vascular disease.

Acknowledgments. The authors thank Vince Segovia for his contribution to this article as a photographer.

References

1. Cho M, Kiss S. Detection and monitoring of sickle cell retinopathy using ultra wide-field color photography and fluorescein angiography. *Retina* 2011;31:738–47.
2. Wessel MM, Aaker GD, Parlitsis G, et al. Ultra-wide-field angiography improves the detection and classification of diabetic retinopathy. *Retina* 2012;32:785–91.
3. Heussen FM, Tan CS, Sadda SR. Prevalence of peripheral abnormalities on ultra-widefield greenlight (532 nm) autofluorescence imaging at a tertiary care center. *Invest Ophthalmol Vis Sci* 2012;53:6526–31.
4. Silva PS, Cavallerano JD, Sun JK, et al. Nonmydriatic ultra-wide field retinal imaging compared with dilated standard 7-field 35-mm photography and retinal specialist examination for evaluation of diabetic retinopathy. *Am J Ophthalmol* 2012;154:549–59.
5. Tan CS, Heussen F, Sadda SR. Peripheral autofluorescence and clinical findings in neovascular and non-neovascular age-related macular degeneration. *Ophthalmology* 2013;120:1271–7.
6. Spaide RF. Peripheral areas of nonperfusion in treated central retinal vein occlusion as imaged by wide-field fluorescein angiography. *Retina* 2011;31:829–37.
7. Singer M, Tan CS, Bell D, Sadda SR. Area of peripheral retinal nonperfusion and treatment response in branch and central retinal vein occlusion. *Retina* 2014;34:1736–42.
8. Patel RD, Messner LV, Teitelbaum B, et al. Characterization of ischemic index using ultra-widefield fluorescein angiography in patients with focal and diffuse recalcitrant diabetic macular edema. *Am J Ophthalmol* 2013;155:1038–44.

9. Wessel MM, Nair N, Aaker GD, et al. Peripheral retinal ischemia, as evaluated by ultra-widefield fluorescein angiography, is associated with diabetic macular oedema. *Br J Ophthalmol* 2012;96:694–8.
10. Sim DA, Keane PA, Rajendram R, et al. Patterns of peripheral retinal and central macular ischemia in diabetic retinopathy as evaluated by ultra-widefield fluorescein angiography. *Am J Ophthalmol* 2014;158:144–53.
11. Prasad PS, Oliver SC, Coffee RE, et al. Ultra wide-field angiographic characteristics of branch retinal and hemicentral retinal vein occlusion. *Ophthalmology* 2010;117:780–4.
12. Croft DE, van Hemert J, Wykoff CC, et al. Precise montage and metric quantification of retinal surface area from ultra-widefield fundus photography and fluorescein angiography. *Ophthalmic Surg Lasers Imaging Retina* 2014;45:312–7.
13. Sagong M, van Hemert J, Olmos de Koo LC, et al. Assessment of accuracy and precision of quantification of ultra-widefield images. *Ophthalmology* 2015;122:864–6.
14. Escudero-Sanz I, Navarro R. Off-axis aberrations of a wide-angle schematic eye model. *J Opt Soc Am A Opt Image Sci Vis* 1999;16:1881–91.
15. Nicholson BP, Nigam D, Miller D, et al. Comparison of wide-field fluorescein angiography and 9-field montage angiography in uveitis. *Am J Ophthalmol* 2014;157:673–7.
16. Tan CS, Chew MC, van Hemert J, et al. Measuring the precise area of peripheral retinal non-perfusion using ultra-widefield imaging and its correlation with the ischaemic index. *Br J Ophthalmol* 2016;100:235–9.
17. Samarawickrama C, Hong T, Jonas JB, Mitchell P. Measurement of normal optic nerve head parameters. *Surv Ophthalmol* 2012;57:317–36.
18. Rutnin U, Schepens CL. Fundus appearance in normal eyes. II. The standard peripheral fundus and developmental variations. *Am J Ophthalmol* 1967;64:840–52.
19. Asdourian GK, Goldberg ME. The angiographic pattern of the peripheral retinal vasculature. *Arch Ophthalmol* 1979;97:2316–8.
20. Wise GN, Dollery CT, Henkind P. *The Retinal Circulation*. New York: Harper; 1971:1–18.
21. Blair MP, Shapiro MJ, Hartnett ME. Fluorescein angiography to estimate normal peripheral retinal nonperfusion in children. *J AAPOS* 2012;16:234–7.
22. Imasawa M, Morimoto T, Iijima H. Recovery of visual field loss due to central retinal artery occlusion. *Jpn J Ophthalmol* 2004;48:294–9.
23. Spitznas M, Bornfeld N. The architecture of the most peripheral retinal vessels. *Albrecht Von Graefes Arch Klin Exp Ophthalmol* 1977;203:217–29.
24. Taylor E, Jennings A. Calculation of total retinal area. *Br J Ophthalmol* 1971;55:262–5.
25. Karampelas M, Sim DA, Chu C, et al. Quantitative analysis of peripheral vasculitis, ischemia, and vascular leakage in uveitis using ultra-widefield fluorescein angiography. *Am J Ophthalmol* 2015;159:1161–8.
26. Silva PS, Dela Cruz AJ, Ledesma MG, et al. Diabetic retinopathy severity and peripheral lesions are associated with nonperfusion on ultrawide field angiography. *Ophthalmology* 2015;122:2465–72.
27. Kaneko Y, Moriyama M, Hirahara S, et al. Areas of non-perfusion in peripheral retina of eyes with pathologic myopia detected by ultra-widefield fluorescein angiography. *Invest Ophthalmol Vis Sci* 2014;55:1432–9.

Footnotes and Financial Disclosures

Originally received: November 12, 2015.

Final revision: January 12, 2016.

Accepted: January 13, 2016.

Available online: ■■■■.

Manuscript no. 2015-2008.

¹ Department of Ophthalmology, Medical Center Ophthalmology Associates, San Antonio, Texas.

² Doheny Eye Institute, Department of Ophthalmology, David Geffen School of Medicine at UCLA, Los Angeles, California.

³ Department of Ophthalmology, Yeungnam University College of Medicine, Daegu, South Korea.

⁴ Optos Plc, Dunfermline, United Kingdom.

⁵ Institute for Ophthalmic Research, Center for Ophthalmology, Eberhard Karls University Tuebingen, Tuebingen, Germany.

Presented at: Macula Society, February 2015, Scottsdale, Arizona; and at Euretina, September 2015, Nice, France.

*Both Dr. Singer and Dr. Sagong contributed equally as first authors.

Financial Disclosure(s):

The author(s) have made the following disclosure(s): M.S.: Consultant and Financial support - Optos (Dunfermline, UK)

J.v.H.: Patents - Optos PLC

S.R.S.: Consultant and Financial support - Carl Zeiss Meditec (Dublin, CA) and Optos (Dunfermline, UK)

M.S.: Research grant -Yeungnam University, Daegu, South Korea

Author Contributions:

Conception and design: Singer, Sadda

Analysis and interpretation: Singer, Sagong, van Hemert, Kuehlewein, Bell, Sadda

Data collection: Singer, Sagong, van Hemert, Kuehlewein, Bell, Sadda

Obtained funding:

Overall responsibility: Singer, Sagong, Sadda

Abbreviations and Acronyms:

D = diopter; **DD** = disc diameter; **FA** = fluorescein angiography; **ICC** = interclass correlation coefficient; **UWF** = ultra-widefield.

Correspondence:

SriniVas R. Sadda, MD, Doheny Eye Institute, Department of Ophthalmology, David Geffen School of Medicine at UCLA, 1450 San Pablo Street, DEI 3623, Los Angeles, CA 90033. E-mail: SSadda@doheny.org.